Vertically Aligned Carbon Nanofibers Coupled with Organosilicon Electrolytes: Electrical Properties of a High-Stability Nanostructured Electrochemical Interface

Kiu-Yuen Tse, Lingzhi Zhang, Sarah E. Baker, Beth M. Nichols, Robert West, and Robert J. Hamers*

Department of Chemistry, University of Wisconsin—Madison, 1101 University Avenue, Madison, Wisconsin 53706

Received June 1, 2007

Organosilicon compounds can form novel electrolytes having a number of unusual properties, including high electrochemical stability, high thermal stability, and low viscosity. Vertically aligned carbon nanofibers can act as exceptionally good nanostructured electrodes, with the vertical orientation and presence of edge-plane graphite along the sidewalls providing desirable electrochemical properties. We have explored the electrical properties of the interfaces of VACNF electrodes with a model organosilicon electrolyte solution. The compound 1-(3-{2-[2-(2-methoxy-ethoxy)-ethoxy]-ethoxy}-propyl)-1,1,3,3,3-pentamethyl-disiloxane (2SM3) with added lithium bis-oxalato-borate (LiBOB) was used. Forests of vertically aligned carbon nanofibers (VACNFs) ∼80 nm in diameter grown by plasma-enhanced chemical vapor deposition (PECVD) were used as electrodes. Our results show that the resulting interfaces yield interfacial capacitances equal to the increase in geometric area, indicating full electrochemical accessibility of the nanofiber sidewalls. Measurements as a function of potential perfect stability at applied voltages up to 3 V. Some initial Faradaic reactions arise near 3.5 V, but these decrease within a few cycles to produce interfaces that exhibit excellent stability up to 5 V while yielding >1000 μF/cm^2 from nanofibers only 2 μm long. The results show that the organosilicon electrolyte combined with VACNFs provides excellent electrochemical properties. The results have implications for understanding the ability to integrate organosilicon electrolytes with high-surface-area carbon materials for applications such as electrochemical double-layer capacitors and lithium-ion batteries.

Introduction

Electrochemical interfaces of nanostructured carbon-based materials with nonaqueous electrolytes are playing increasingly important roles in a number of existing and emerging technologies for storage and conversion of energy, such as electrochemical double layer capacitors (EDLC) and lithium-ion batteries. Interfaces of carbon with organic electrolytes based on acetonitrile and alkyl carbonates have been widely studied.[1−6] However, the flammability and limited range of electrochemical stability of these compounds remain a limiting factor.[1,3,4,7] These issues have increased interest in alternative materials such as ionic liquids.[3] Organosilicon electrolytes have recently emerged as an novel class of materials that have high dielectric constants and high ionic conductivity,[8−11] along with relatively low viscosity. Moreover, their low flammability[12] suggests they may be good alternatives to more commonly used electrolytes.

Recent studies have characterized the interaction of organosilicon electrolytes with planar electrodes made from highly oriented pyrolytic graphite[13,14] However, most practical applications require use of some form of nanostructured carbon to provide high surface areas and high electrochemical stability. Nanostructured carbon provides high chemical stability and high surface area.[15−17] However, with conventional porous carbons, much of that area is not electrically accessible because of limitations of ion transport within small pores.[1,18] Vertically aligned carbon nanofibers (VACNFs)[19−22] are of interest because the vertical orientation of the

* Corresponding author. E-mail: rjhamers@wisc.edu. Phone: (608) 262-6371.

(1) Frackowiak, E.; Beguin, F. *Carbon* **2001**, *39*, 937.
(2) Frackowiak, E.; Gautier, S.; Gaucher, S.; Bonnamy, S.; Beguin, F. *Carbon* **1999**, *37*, 61.
(3) Frackowiak, E.; Lota, G.; Pernak, J. *Appl. Phys. Lett.* **2005**, *86*, 164104.
(4) Morimoto, T.; Hiratsuka, K.; Sanada, Y.; Kurihara, K. *J. Power Sources* **1996**, *60*, 239.
(5) Portet, C.; Taberna, P. L.; Simon, P.; Flahaut, E.; Laberty-Robert, C. *Electrochim. Acta* **2005**, *50*, 4174.
(6) Fang, B.; Binder, L. *J. Phys. Chem. B* **2006**, *110*, 7877.
(7) Xu, K.; Ding, M. S.; Zhang, S. S.; Allen, J. L.; Jow, T. R. *J. Electrochem. Soc.* **2003**, *150*, A161.
(8) Lyons, L.; Morcom, K.; Schneider, Y.; Zhang, X.; Rossi, N. A.; West, R. *PMSE Prepr.* **2005**, *92*, 443.
(9) Rossi, N. A. A.; Zhang, Z.; Wang, Q.; Amine, K.; West, R. *Polym. Prepr. (Am. Chem. Soc., Div. Polym. Chem.)* **2005**, *46*, 723.
(10) Zhang, Z.; Rossi, N. A. A.; Olson, C.; Wang, Q.; Amine, K.; West, R. *Polym. Prepr. (Am. Chem. Soc., Div. Polym. Chem.)* **2005**, *46*, 662.
(11) Zhang, Z.; Rossi, N. A. A.; Simon, A.; Wang, Q.; Amine, K.; West, R. *PMSE Prepr.* **2005**, *92*, 365.
(12) Buch, R. R. *Fire Saf. J.* **1991**, *17*, 1.
(13) Nakahara, H.; Nutt, S. *J. Power Sources* **2006**, *160*, 1355.
(14) Nakahara, H.; Yoon, S.; Nutt, S. *J. Power Sources* **2006**, *160*, 548.
(15) Lin, Y.; Taylor, S.; Li, H. P.; Fernando, K. A. S.; Qu, L. W.; Wang, W.; Gu, L. R.; Zhou, B.; Sun, Y. P. *J. Mater. Chem.* **2004**, *14*, 527.
(16) Ajayan, P. *Chem. Rev.* **1999**, *99*, 1787.
(17) Katz, E.; Willner, I. *ChemPhysChem* **2004**, *5*, 1084.
(18) de Levie, R. *Electrochim. Acta* **1964**, *9*, 1231.
(19) Melechko, A. V.; Merkulov, V. I.; McKnight, T. E.; Guillorn, M. A.; Klein, K. L.; Lowndes, D. H.; Simpson, M. L. *J. Appl. Phys.* **2005**, *97*, 041301.

10.1021/cm0714842 CCC: $37.00
Published on Web 10/13/2007

nanofibers may provide especially good accessibility to species in solution,[23] whereas the direct bonding of each individual nanofiber to the underlying electrode provides low-resistance connections. Carbon nanofibers grown using a nickel catalyst are formed in a nested-cup structure in which graphitic edge planes are exposed at the sidewalls.[19,24,25] Because graphitic edge planes have been shown to exhibit ~30 times higher capacitance and orders of magnitude higher electron-transfer rates than basal planes,[26,27] this suggest that nanofibers may be excellent electrode materials for use with organosilicon electrolytes.

Here, we report investigations of the interfacial electrical properties of vertically aligned carbon nanofibers in a model organosilicon electrolyte, 1-(3-{2-[2-(2-Methoxy-ethoxy)-ethoxy]-ethoxy}-propyl)-1,1,3,3,3-pentamethyl-disiloxane (2SM3). Our results demonstrate that organosilicon electrolyte can effectively take advantage of the high surface area of VACNF electrodes, providing a number of excellent electrochemical properties, including stability over extended voltage ranges and good high-frequency response. These results suggest that organosilicon electrolyte interfaces to nanostructured carbons may be attractive candidates for potential applications in electrochemical energy storage devices.

2. Experimental Methods

2.1. Growth and Characterization of Carbon Nanofibers. Vertically aligned carbon nanofibers were grown using DC plasma-enhanced chemical vapor deposition (PECVD)[19,21,28,29] in a custom-built chamber. Nanofibers were grown on planar substrates that were covered with a thin multilayer film consisting of 40 nm of molybdenum, followed by 20 nm of titanium, and finally 20 nm nickel as the top layer. Several different types of substrates were used (including planar silicon wafers and stainless-steel disks) with equivalent results. Typical growth conditions used flow rates of 100 standard cubic centimeters per minute (sccm) ammonia and 30 sccm acetylene, with a chamber pressure of 4 Torr and a DC power of 360 W. Figure 1a shows a scanning electron microscope image of the resulting carbon nanofibers. Under our growth conditions, the nanofibers are nearly cylindrical and are nearly all vertically aligned. Analysis of higher-resolution SEM images yields an average diameter of 80 nm. The length of the nanofibers can be controlled by varying the duration of the growth. Nanofibers reported here were obtained with a growth time of 20−30 min, which yields fibers with an average length of 2−3 μm. In some experiments, the nickel catalyst was removed by exposing the VACNFs to a brief plasma of pure NH_3, and then immersing in a solution containing Fe^{3+} ion or using electrochemical oxidation. However, we found catalyst removal to have no effect on the electrical properties. We believe this can be attributed to the fact that the Ni catalyst of the as-grown VACNFs is covered with a thin layer of carbon that acts as an impervious barrier. Indeed, we found that immersion of as-grown nanofibers into highly oxidizing solutions such as Fe^{3+} would not remove the Ni catalyst; removal was only possible after briefly etching the VACNFs in a plasma of NH_3 or other suitable etchant.

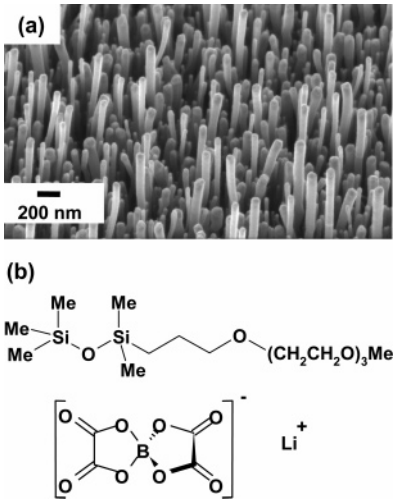

Figure 1. Structures of nanofibers and electrolyte components. (a) Scanning electron microscope (SEM) image of vertically aligned carbon nanofiber electrode. (b) Structures of organosilicon electrolyte and of the lithium salt. Upper panel: 1-(3-{2-[2-(2-Methoxy-ethoxy)-ethoxy]-ethoxy}-propyl)-1,1,3,3,3-pentamethyl-disiloxane (2SM3). Lower panel: Lithium bis-oxalato-borate (LiBOB).

VACNF electrodes were characterized with X-ray photoelectron spectroscopy (XPS) and ultraviolet photoelectron spectroscopy (UPS). These measurements were performed in an ultrahigh vacuum Physical Electronics system equipped with a monochromatized K_α source (1486.6 eV) and a He(I) resonance lamp (21.2 eV).

2.2. Synthesis of Organosilicon Electrolyte. The organosilicon electrolyte used was 1-(3-{2-[2-(2-methoxy-ethoxy)-ethoxy]-ethoxy}-propyl)-1,1,3,3,3-pentamethyl-disiloxane (referred to here as 2SM3), as shown in Figure 1b. The salt lithium bis-oxalato-borate (LiBOB), also shown in Figure 1b, can be readily dissolved to yield a 0.8 M solution with low viscosity (3.8 centipoise at 300 K), moderate dielectric constant (4.3), and high ionic conductivity (3.65×10^{-4} S/cm).[8−11] 2SM3 was synthesized through a hydrosilylation reaction of pentamethyldisiloxane with allyl tri(ethylene glycol)monomethyl ether using Karlstedt's catalyst, as reported elsewhere.[11]

2.3. Electrical Characterization. Electrical properties were characterized using electrical impedance spectroscopy (EIS), cyclic voltammetry (CV), and galvanostatic experiments. The electrochemical cells were fabricated by sandwiching a piece of polyethylene−polypropylene trilayer Celgard separator containing the organosilicon electrolyte between two opposing carbon nanofiber electrodes in a sealed two-electrode Teflon cell. All experiments were performed at room temperature. Electrochemical measurements were performed using a potentiostat (Solartron 1260) and impedance analyzer (Solartron 1287) using Corrware and Zplot software (Scribner Associates, Inc).

Impedance spectroscopy measurements[30] used a 10 mV AC modulation to obtain the real and imaginary parts of the complex

(20) Melechko, A. V.; McKnight, T. E.; Hensley, D. K.; Guillorn, M. A.; Borisevich, A. Y.; Merkulov, V. I.; Lowndes, D. H.; Simpson, M. L. *Nanotechnology* **2003**, *14*, 1029.
(21) Meyyappan, M.; Delzeit, L.; Cassell, A.; Hash, D. *Plasma Sources Sci. Technol.* **2003**, *12*, 205.
(22) Kim, T.; Lim, S.; Kwon, K.; Hong, S.-H.; Qiao, W.; Rhee, C. K.; Yoon, S.-H.; Mochida, I. *Langmuir* **2006**, *22*, 9086.
(23) Li, J.; Cassell, A.; Delzeit, L.; Han, J.; Meyyappan, M. *J Phys. Chem. B* **2002**, *106*, 9299.
(24) Banks, C. E.; Compton, R. G. *Analyst* **2006**, *131*, 15.
(25) Banks, C. E.; Davies, T. J.; Wildgoose, G. G.; Compton, R. G. *Chem. Commun.* **2005**, 829.
(26) Rice, R. J.; Mccreery, R. L. *Anal. Chem.* **1989**, *61*, 1637.
(27) Robinson, R. S.; Sternitzke, K.; McDermott, M. T.; McCreery, R. L. *J. Electrochem. Soc.* **1991**, *138*, 2412.
(28) Ren, Z. F.; Huang, Z. P.; Xu, J. W.; Wang, J. H.; Bush, P.; Siegal, M. P.; Provencio, P. N. *Science* **1998**, *282*, 1105.
(29) Cassell, A. M.; Ye, Q.; Cruden, B. A.; Li, J.; Sarrazin, P. C.; Ng, H. T.; Han, J.; Meyyappan, M. *Nanotechnology* **2004**, *15*, 9.
(30) Macdonald, J. R.; Kenan, W. R. *Impedance Spectroscopy—Emphasizing Solid Materials and Systems*; John Wiley: New York, 1987.

impedance, defined as $\hat{Z} = \hat{V}/\hat{I} = Z' + iZ''$. Impedance data are presented as the magnitude ($|Z|$) and phase angle (θ) of the impedance as a function of frequency f and in some cases as Nyquist plots, in which the real (Z') and imaginary (Z'') components are plotted on a single graph. The capacitance of the system can be extracted from the imaginary part using

$$C = -\frac{1}{2\pi f Z''} \tag{1}$$

assuming a series RC model.

3. Results

3.1. Physical Characterization of VACNF Electrodes. Previous studies have shown that electron-transfer rates and interfacial capacitance of carbon-based materials are strongly dependent on the hybridization and crystallographic orientation of the carbon that is used.[26,27,31−33] Transmission electron microscope images (not shown) confirm that our nanofibers have a stacked-cup structure in which graphitic edge planes are exposed every 2−3 nm along the length of the fiber. To explore the electronic properties, we characterized our VACNF electrodes using X-ray photoelectron spectroscopy (XPS) and ultraviolet photoemission spectroscopy (UPS). Figure 2a shows an XPS survey spectrum of as-grown VACNF electrodes. The spectrum shows a strong C(1s) peak near 285 eV and a small trace of nitrogen, visible as a small peak near 400 eV. A high-resolution scan of the C(1s) region (Figure 2b) shows a main peak at 285 eV and a characteristic "shakeup" peak near 291 eV; this broad peak arises the excitation of a $\pi-\pi^*$ transition during photoelectron ejection and is a characteristic signature of a conjugated π-electron system.[34] The clear appearance of this peak shows that the outermost regions of the nanofibers have a high degree of π conjugation.

Figure 2c shows ultraviolet photoelectron spectroscopy (UPS) data for VACNF electrodes, using the He(I) source (21.2 eV) for excitation. The most important feature in this spectrum is the persistence of significant photoelectron emission all the way to the Fermi energy at 0 V. The high photoelectron emission implies that there is a high density of states all the way to E_F and strongly suggests that the VACNF electrodes have a metalliclike electronic structure.

3.2. Electrical Impedance of the VACNF−Organosilicon Interface. Figure 3 shows the impedance spectra of a VACNF sample along with a control sample of glassy carbon, in 2SM3 solutions containing 0.8 M LiBOB at 0 V bias. The experimental data are indicated with the markers, whereas the lines show the results of fitting to the equivalent circuit model in Figure 3e. Figure 3a shows the magnitude of the impedance for these two samples, whereas Figure 3b shows the phase. At the lowest frequencies measured (3 mHz), the impedance of the VACNF sample is very high, $\sim 1 \times 10^5\ \Omega\ \text{cm}^2$. As the frequency is increased, the impedance immediately begins to decrease until it reaches a plateau at frequencies above ~100 Hz. The nanofiber sample exhibits a phase angle of approximately −83° between 0.01 Hz and ~20 Hz, decreasing toward zero at higher and lower frequencies. At frequencies >100 Hz, the measured impedance is dominated by the resistance of the electrolyte.

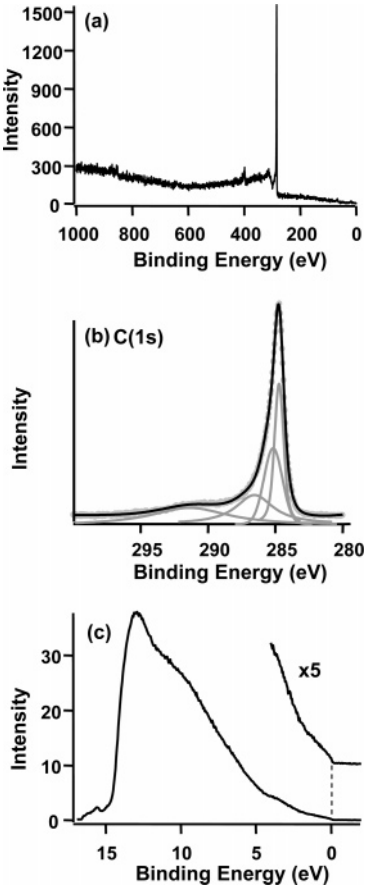

Figure 2. XPS and UPS of carbon nanofibers. (a) X-ray photoelectron survey spectrum. (b) High-resolution C(1s) spectrum. (c) Ultraviolet photoelectron spectrum, inset is a 5× magnification of the region close to Fermi level.

For comparison, Figure 3 also shows similar data measured using a glassy carbon electrode in 2SM3. The impedance of the glassy carbon sample is nearly constant at frequencies below ~0.05 Hz, but decreases at higher frequencies. The phase behavior is somewhat complex, starting with a phase angle of approximately −13° at the lowest frequency measured (8 mHz), increasing to a maximum value of −59° at 1 Hz, and then decreasing again to −34° at 10 kHz. These results on glassy carbon are very similar to a recent report on 2SM3 interfacing with planar highly oriented pyrolytic graphite (HOPG) electrodes.[14]

The impedance properties can be modeled at varying degrees of complexity. Figure 3c shows the effective capacitance extracted from the imaginary part of the impedance using eq 1. For both samples, the effective capacitance decreases monotonically with increasing frequency, though the nanofiber sample has a much smaller frequency dependence. In 2SM3, the nanofiber samples yields a capacitance at least an order of magnitude higher than the control sample over most of the frequency range. The glassy carbon sample shows a sharper increase in apparent capacitance at frequencies below ~0.1 Hz; as discussed later, this is not a true

(31) Kneten, K. R.; McCreery, R. L. *Anal. Chem.* **1992**, *64*, 2518.
(32) Cline, K. K.; Mcdermott, M. T.; Mccreery, R. L. *J. Phys. Chem.* **1994**, *98*, 5314.
(33) McDermott, M. T.; McDermott, C. A.; McCreery, R. L. *Anal. Chem.* **1993**, *65*, 937.
(34) Jackson, S.; Nuzzo, R. *Appl. Surf. Sci.* **1995**, *90*, 195.

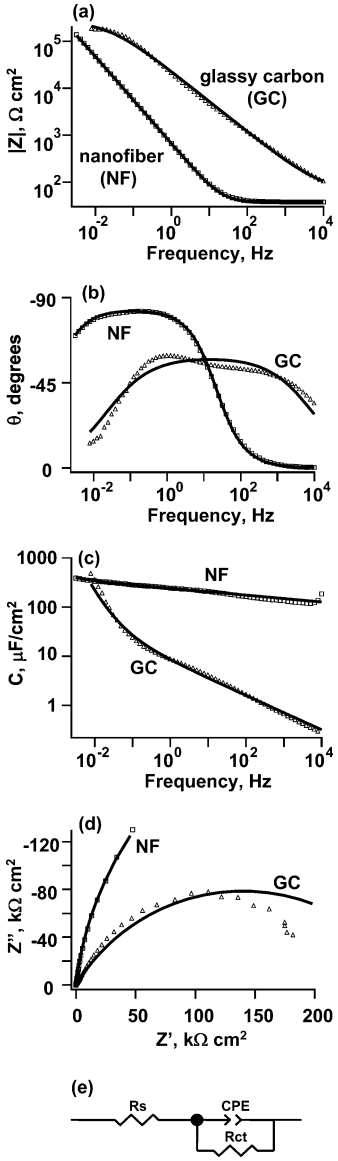

Figure 3. Electrical impedance spectra of nanofibers in the electrolyte 2SM3 containing 0.8 M LiBOB, along with a control sample of glassy carbon in the same solution, lines are fit results. (a) absolute impedance vs frequency. (b) Phase angle vs frequency. (c) Capacitance vs frequency. (d) Nyquist plot. (e) Equivalent circuit used in fitting the data in Figure 2a−d.

increase in capacitance but is a result of Faradaic processes whose effects becomes apparent at low frequency where the impedance associated with the double-layer capacitance becomes very high. The solid line shows a fit to the more elaborate model shown in Figure 3e, and then an extractiion of the equivalent series capacitance from the complex impedance data.

Figure 3d shows the Nyquist plot of the same data presented in Figure 3a−c. The nanofiber sample presents almost a straight line at a small angle to the *y*-axis, indicating a close to ideal capacitive behavior. The glassy carbon sample gives a semicircle, indicating parallel RC circuit components dominating the impedance in the measured frequency range.

The plots in Figure 3 also include fits of the experimental data to the circuit model shown in Figure 3e. Although many models are possible, this model gives a reasonably good fit to all the data and makes physical sense. This model is a slight modification of the widely used Randles cell[35] except that it uses a constant phase element (CPE), instead of a capacitor, to represent the double-layer capacitance. The CPE is defined by the impedance relationship

$$\hat{Z} = \frac{1}{T(i\omega)^P} \tag{2}$$

and is often employed to account for deviations from ideal capacitive behavior due to microscopic roughness or other factors.[30] Using the area-normalized impedance Z (with units of Ω cm²), T has units of $1/(\mathrm{Hz}^p\ \Omega\ c\mathrm{m}^2)$ and is in units of farads when $P = 1$. R_s represents the uncompensated solution resistance and R_{ct} represents the large but finite interfacial charge-transfer resistance. The fit results are represented by solid lines in Figure 3a−d, and the component values are shown in Table 1. Table 1 shows that the nanofiber sample exhibits a CPE-P value of 0.93, whereas the value on glassy carbon is 0.65; this shows that the nanofiber interface behaves more ideally as a capacitor. Although CPE-T values cannot be compared as capacitance directly because of the difference in dimensionality (vide infra), a numerical comparison gives a rough idea of the difference in capacitance.

Table 1. Results of Fitting the Data in Figure 3a−d to the Circuit Model in Figure 3e

	CPE-T	CPE-P	R_{ct} (kΩ cm²)	R_s (Ω cm²)
nanofibers	$(273 \pm 1) \times 10^{-6}$	0.930 ± 0.001	556 ± 17	38.0 ± 0.1
glassy carbon	$(12.8 \pm 0.3) \times 10^{-6}$	0.652 ± 0.004	280 ± 13	62.6 ± 4.1

The data in Figure 3 show that at frequencies between ∼3 mHz and 20 Hz, the total impedance is dominated by the interfacial capacitance, whereas at high frequencies, it is dominated by the electrolyte resistance. The results in Table 1 indicate that the nanofiber surface has a capacitance about 20 times higher than the glassy carbon control sample. The very small dependence on frequency, as reflected in the CPE-P value of 0.93 (close to unity) shows that the nanofiber−electrolyte interface behaves as a nearly idea capacitor. A more quantitative analysis of the data will be presented later in the paper.

Figure 4 shows the results of similar experiments carried in a 0.8 M aqueous potassium chloride solution. The experimental data are indicated with the markers, whereas the lines show the results of fitting to the equivalent circuit model in Figure 3e. The nanofiber sample again shows a steady decrease in impedance with frequency over most of the frequency range. At the lowest frequencies it reaches a plateau of ∼6000 Ω cm² (and a phase angle near zero) that can be attributed to a parallel leakage resistance, whereas at the highest frequencies it reaches a limiting impedance of several Ω cm² because of solution resistance. Figure 4c shows the interfacial capacitance extracted from these data using a series RC model. The nanofibers show a larger capacitance and more uniform frequency response when compared with the glassy carbon sample.

Comparing the data in 2SM3 (Figure 3) with that in aqueous KCl (Figure 4) shows some significant differences. Carbon nanofibers in 2SM3 (Figure 3) show an almost ideal

(35) Randles, J. E. B. *Discuss. Faraday Soc.* **1947**, *1*, 11.

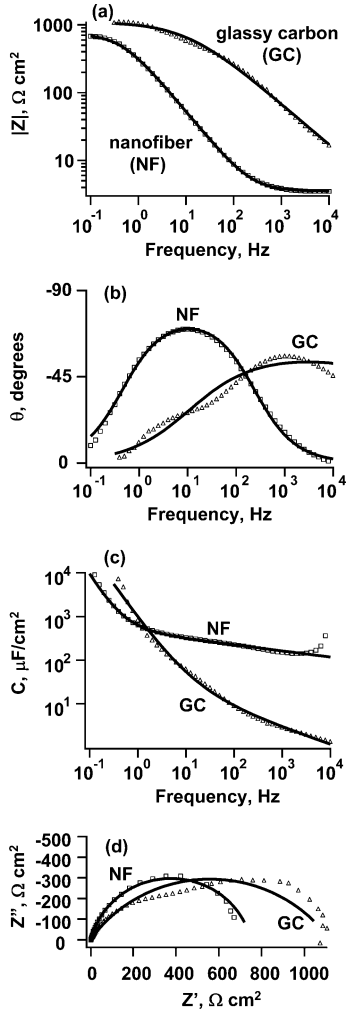

Figure 4. Electrical impedance spectra of nanofibers in 0.8 M aqueous potassium chloride solution, along with a control sample of glassy carbon in the same solution, lines are fit results. (a) Absolute impedance vs frequency. (b) Phase angle vs frequency. (c) Capacitance vs frequency. (d) Nyquist plot.

Table 2. Results of Fitting the Data in Figure 4a−d to the Circuit Model in Figure 3e

	CPE-T	CPE-P	R_{ct} (kΩ cm^2)	R_s (Ω cm^2)
nanofibers	$(542 \pm 7) \times 10^{-6}$	0.860 ± 0.003	745 ± 8	3.49 ± 0.03
glassy carbon	$(65.3 \pm 3.9) \times 10^{-6}$	0.618 ± 0.009	1120 ± 26	1.05 ± 0.85

1/*f* frequency dependence at low frequencies, whereas in KCl, the impedance plateaus at frequencies lower than ∼1 Hz because of Faradaic reactions. The less-than-ideal capacitive behavior of the nanofiber−KCl interface is also reflected in decrease in phase angle toward 0° at frequencies <1 Hz. The nanofiber−organosilicon interface shows a straight line (characteristic of nearly perfect capacitive behavior) in the Nyquist plot down to very low frequencies, whereas the nanofiber−KCl interface shows a semicircle characteristic of a parallel RC circuit. Table 2 shows the numerical fit results. The trends are similar to those in organosilicon electrolyte, whereas the nanofiber−KCl interface shows a CPE-P value closer to 1 and hence a more ideal capacitive behavior comparing to the glassy carbon−KCl interface, and a CPE-T value an order of magnitude higher. Another notable difference is that the nanofibers in KCl show a solution

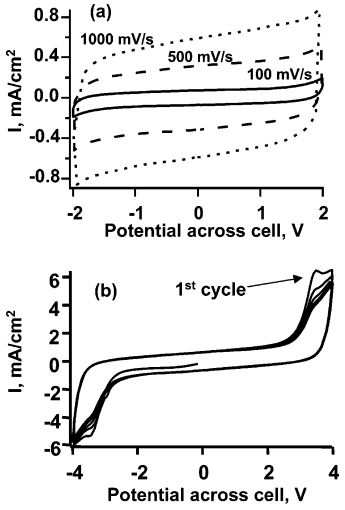

Figure 5. Cyclic voltammetric studies of carbon nanofiber−organosilicon electrolyte interface. (a) Cyclic voltammograms at different scan rates. (b) Cyclic voltammogram up to ± 4 V; scan rate, 500 mV/s.

resistance R_s of ∼3.5 Ω cm^2 that is more than 10 times lower than that in the organosilicon electrolyte (38 Ωcm^2). This is significant because it shows that the resistance of 38 Ω cm^2 observed for nanofibers in 2SM3 does not arise from the nanofibers or the underlying electrode structures, but must be associated with the 2SM3/LiBOB electrolyte.

3.3. Capacitance and Voltage Stability of VACNF/Organosilicon Interface. To investigate the electrochemical behavior away from the open circuit potential, we conducted cyclic voltammetry experiments. Because of the difficulty of obtaining a reliable reference electrode that would work in 2SM3, these measurements were limited to a two-electrode configuration, using two identical VACNF electrodes. Figure 5a shows results over a ± 2 V potential window at three different scan rates. The *I*−*V* responses all show a rectangular shape that is typical of capacitors, even at a high scan rate of 1000 mV/s and up to a ± 2 V potential window. The capacitance of each electrode is given by

$$C = \frac{2i}{\Delta\upsilon/\Delta t} \tag{3}$$

where *i* is the current density (current per unit area) and $\Delta\upsilon/\Delta t$ is the scan rate. The factor of 2 in the numerator arises from the symmetric design of the electrochemical cell, which uses two identical samples as electrodes. From the voltammogram, we obtained a capacitance of 1440 μF/cm^2 at a scan rate of 100 mV/s. When the scan rates were increased to 500 and 1000 mV/s, the capacitance drops only slightly to 1270 and 1180 μF/cm^2, respectively. The absence of any redox peaks in this potential window demonstrates that there are no significant faradaic reactions under these conditions.

Figure 5a shows that the capacitance values are perfectly stable over a voltage range of −2 to +2 V. At higher voltages, Figure 5b shows excellent stability up to at least 3.2 V, with small oxidation and reduction peaks are observed when the applied voltage reaches 3.5 V. These reactions are irreversible, and the 3.5 V peaks slowly disappear with repeated cycles. Although the exact chemical origin of these reactions is yet unknown, repeated measurements show rectangular *I*−*V* curves up to a very high scan rate of 5000

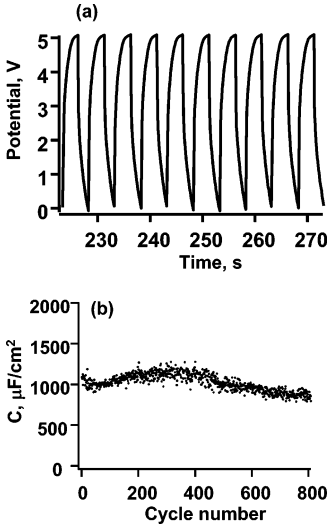

Figure 6. Galvanostatic studies of carbon nanofiber−organosilicon electrolyte. (a) A segment of the constant current charging and discharging curve showing 10 cycles; current, 500 μA; electrode area, 0.95 cm^2. (b) Normalized capacitance per electrode vs cycle numbers.

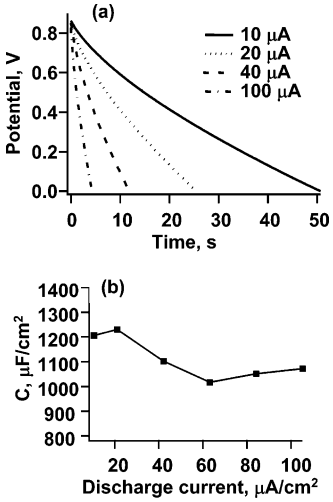

Figure 7. Influence of discharge current on capacitance of carbon nanofiber−organosilicon electrolyte interface. (a) Galvanostatic discharge curves for different discharge current; sample area, 0.95 cm^2. (b) Normalized capacitance per electrode as a function of discharge current density.

mV/s and up to a potential window of ± 3 V. Even at voltages as high as ± 4 V as shown in Figure 5b, the peaks disappeared about a few cycles and the cyclic voltammograms become stable after the first few cycles.

3.4. Galvanostatic Studies. The results in Figure 5 suggest that although nanofiber interfaces with the organosilicon electrolyte 2SM3/LiBOB show some initial decomposition at voltages >3 V, this decomposition is self-limiting, forming an interface that exhibits higher stability than that of the bare nanofibers. To test the longer-term stability of the interface, we conducted experiments in which a cell made from nanofiber electrodes with 2SM3/LiBOB was repeatedly charged and discharged with a constant current of 500 μA between 0 and 5 V for 800 cycles; each cycle takes approximately 5 s. Figure 6a is an arbitrarily chosen segment of the charge−discharge curve showing 10 cycles. Figure 6b shows the calculated capacitance using eq 3 vs cycle number. The capacitance is quite stable over the entire 800 cycles (~4000 s) of the experiment, showing only a slight increase from ~1000 to ~1100 μF/cm^2 and then a small decline to ~900 μF/cm^2. Thus, we conclude that although some faradaic current is observed above 3V (Figure 5b), the nanofiber−organosilicon electrolyte interface is generally stable with repeated cycling up to voltages of 5 V.

Figure 7 shows discharging experiments in compound 2SM3 as a function of discharge current. In this set of experiments, the interface was charged at 0.9 V for 30 s, and then discharged at a constant current while monitoring the total cell potential vs time (Figure 7a). The capacitance can again be calculated with eq 3 using the voltage drop in the linear region.[36,37] Figure 7b shows that the capacitance drops only slightly from 1200 to ~1000−1100 μF/cm^2 as the discharge current is increased from 10 to 100 μA/cm^2. The interfacial capacitance is nearly independent of discharge rate, even at the highest discharge currents measured.

(36) An, K.; Kim, W.; Park, Y.; Choi, Y.; Lee, S.; Chung, D.; Bae, D.; Lim, S.; Lee, Y. *Adv. Mater.* **2001**, *13*, 497.
(37) Kim, C.; Yang, K. S. *Appl. Phys. Lett.* **2003**, *83*, 1216.

4. Discussion

Nanofibers as High-Surface-Area Electrodes. One of the principal goals of this work was to understand the electrochemical properties of VACNF electrodes in nonaqueous electrolytes, such as the organosilicon compound 2SM3. The interest in VACNF electrodes largely arises from the fact that the electrical properties of carbon depend strongly on crystal structure and, for graphitic materials, on the exposure of graphitic edge planes. Prior work on highly oriented pyrolitic graphite in aqueous media has shown that the interfacial capacitance of edge-plane graphite is >30 times higher than that of basal-plane graphite (<1 μF/cm^2).[26,33] Single-walled carbon nanotubes have recently been investigated as potential electrode materials, but pristine carbon nanotubes expose only the basal plane of graphite along the sidewalls and therefore must undergo extensive chemical treatment (e.g., oxidation) in order to exhibit good electrochemical properties. In contrast, VACNF electrodes form in a stacked-cup structure that exposes significant amounts of edge-plane graphite along the sidewalls. Transmission electron microscopy images of our samples (not shown) reveal roughly 1 edge-plane site every ~2 nm along the sidewall. This high exposure of edge planes is expected to lead VACNFs to have high interfacial capacitance.

The differences in behavior of various forms of carbon are generally attributed to differences in the density of states near the Fermi energy. Glassy carbon has a high density of states and exhibits a correspondingly high capacitance, on the order of 30−100 μF/cm^2 in 1 M KCl depending on sample preparation.[33] Basal-plane graphite has a low density of states and its interface with an electrolyte leads to a space-charge region within the graphite that is in series with the double-layer capacitance; consequently, the smaller capacitance (that of the graphite) is observed, often <1 μF/cm^2. In contrast, the high density of states of the edge-plane graphite make it behave like a metal.[26,27] Because the nested-cup structure of vertically aligned carbon nanofibers exposes both edge-plane and basal planes, the degree to which a space-

Table 3. Capacitance Values of the Various Interfaces from Eis Data Using Eq 4

	in organosilicon electrolyte 2SM3		in aqueous KCl	
	nanofiber	glassy carbon	nanofiber	glassy carbon
capacitance (μF/cm^2)	397	19.0	462	19.1

charge layer might be formed in the nanofibers can have important consequences for its electrical properties.

The valence-band photoemission data in Figure 2c clearly show that the density of states of the nanofibers is significant all the way up the Fermi energy, and a small but clearly distinct Fermi edge can be seen at the Fermi energy (binding energy = 0). This clearly shows that the nanofibers are metallic in character. The core-level photoemission data show a clear "shakeup" peak near 291 eV that arises from excitation of the graphene π electron system as the electron is ejected. The presence of this peak establishes that the nanofibers are graphitic in character, whereas the high DOS near the Fermi energy shows that the density of states near the Fermi energy is high.

The electrical measurements in Figures 3 and 4 demonstrate that VACNF−organosilicon interfaces have a high effective area and that the sidewalls of the nanofibers are electrically active. As with most porous materials, in order to adequately model the frequency dependence, it is necessary to use a constant phase element (CPE) to account for deviations from ideal capacitive behavior that arise from the three-dimensional nature of the interface. To evaluate the effectiveness of the interfaces for applications in energy storage, it is useful to represent the properties in terms of an effective capacitance. Hsu and Mansfeld[38] derived the following equation to calculate the correct capacitance from CPE-P and CPE-T values

$$C = T(\omega_{max})^{P-1} \quad (4)$$

In this equation, ω_{max} represents the frequency at which the imaginary part of the impedance reaches a maximum, corresponding to the frequency at the top of the depressed semicircle in the Nyquist plot. Using eq 4, we have calculated that the capacitance values of the various interfaces and the results are presented in Table 3. The planar glassy carbon sample in 2SM3 organosilicon electrolyte with 0.8 M LiBOB exhibits a capacitance of (19.0 μF/cm^2) that is nearly identical to that we measure in 0.8 M KCl (19.1 μF/cm^2) and close to the values of 25−50 μF/cm^2 reported previously in ~1 M KCl.[33,39]

The high values of capacitance are significant because previous studies have shown that interfacial capacitance of carbon-based materials is highly dependent on the structure of the material.

Our data show that in the organosilicon electrolyte 2SM3, the nanofiber samples exhibit 21 times higher capacitance than a planar glassy carbon sample, whereas in 0.8 M KCl, the nanofibers exhibit a capacitance 24 times higher than the control sample. These ~20-fold increases in capacitance are very similar to the ~25-fold increase in surface area inferred from SEM image using the measured diameter of 80 nm, length of 2 μm, and measured density ~5 × 10^9 nanofibers/cm^2. Previous measurements on nanofibers grown in a similar manner but slightly shorter in length showed an increase of ~10× in effective surface area as measured by chemical surface adsorption measurements.[40]

The substantial increase in effective capacitance and the agreement between electrical measurements and physical measurements of area suggests that space-charge effects are not significant in the VACNF electrodes, and they behave similarly to metallic electrodes. Because the enhancement in 2SM3/LiBOB is very close to that observed in KCl, we can conclude that although there are inhomogeneities in atomic structure along the nanofiber sidewalls (i.e., edge-plane and basal-plane sites exposed), the net sample area accessible using H_2O/KCl and using 2SM3/LiBOB are similar.

Frequency and Scan-Rate Dependence of the Interfacial Capacitance. Our EIS studies (Figure 3) show that the nanofiber samples, especially in the organosilicon electrolytes, show only a weak dependence on the rate of charging and discharging. The cyclic voltammograms in Figure 5a maintain the rectangular shape even up to a high scan rate of 1000 mV/s (Figure 5a); furthermore, the capacitance is only weakly dependent on the scan rate, decreasing from 1440 μF/cm^2 at 100 mV/s to 1180 μF/cm^2 at 1000 mV/s. Similar conclusions can be reached from the frequency-domain data. The data in Figure 3c show that at the lowest frequency measured (3 mHz) the capacitance is 390 μF/cm^2, and as the frequency increases to 10 kHz, this value drops to 120 μF/cm^2 at 10 kHz. These data demonstrate that the changes in spatial organization of the ions giving rise to the double-layer capacitance can occur very quickly; however, at frequencies above ~100 Hz, the impedance associated with the interfacial capacitance is smaller than the series resistance associated with the 2SM3/LiBOB; hence, the effectiveness for energy storage becomes reduced and instead replaced by energy dissipation due to resistance of the electrolyte. Nevertheless, the observed resistance arises primarily from the electrolyte through the ~25 μm thick spacer between the nanofiber electrodes. In principle, reducing the separation between electrodes could further reduce the series resistance and thereby lead to further improvements in high-frequency response.

Although the capacitance does decrease with increasing frequency (a drop of ~70% in capacitance over 6 orders of magnitude in frequency) and may not be able to be effectively utilized at frequencies >100 Hz (because of the series resistance), the decrease is much smaller than what typically observed with other common high-surface-area carbon-based electrodes such as porous carbons. For porous carbons, the specific capacitances at low frequency are often larger than those reported here, but these high values typically drop rapidly with increasing frequency[5,41−43] because of the

(38) Hsu, C.; Mansfeld, F. *Corrosion* **2001**, *57*, 747.
(39) Swain, G. M. *J. Electrochem. Soc.* **1994**, *141*, 3382.
(40) Baker, S. E.; Tse, K. Y.; Hindin, E.; Nichols, B. M.; Clare, T. L.; Hamers, R. J. *Chem. Mater.* **2005**, *17*, 4971.
(41) Conway, B. E. *Electrochemical Supercapacitors*; Kluwer Academic/Plenum Press: New York, 1999.

distributed resistance that arises within the pores of the material. This distributed resistance within the pores cannot be easily reduced and manifests itself in the constant-phase element as an exponent P of ~0.5,[18] compared with $P \approx 0.93$ we observe for nanofibers in 2SM3/LiBOB. Similarly, previous studies using carbon nanotubes have typically shown that the interfacial capacitance shows a precipitous drop above a "knee frequency" that is typically below 100 Hz and often close to 1 Hz.[5,43,44]

The good frequency response of the VACNFs arises in part from the fact that the vertical alignment provides accessibility of the nanofiber sidewalls to ions in solution, whereas the direct contact of each nanofiber to the underlying electrode provides low resistance. In addition, however, the nanofibers are comparatively short (a few micrometers in thickness), which also reduces the possibility of charging currents being limited by finite rates of diffusion.

Stability of the Nanofiber−Organosilicon Electrolyte Interface. Electrochemical stability and thermal stability of the electrode−electrolyte interface often limits the practical limits of energy storage devices. For example, the energy stored in electrochemical double layer capacitors increases quadratically with voltage, but the practical voltage range is limited to ~1.2 V for aqueous systems and ~2.3 V for symmetric devices (i.e., having identical pairs of electrodes) in organic electrolytes such as acetonitrile or propylene carbonate.[1,3,4] Recently, Frackowiak et al. reported on extending the voltage window to 3.4 V using ionic liquids combining with activated carbon, but to obtain acceptable performance, it was necessary to add acetonitrile.[3] Our data show that pristine VACNF electrodes immersed in 2SM3/LiBOB exhibits stability up to cell voltages of 3.0 V with VACNF electrodes. Very recent studies showed that LiBOB can be reduced at potentials more negative below 1.0 V (vs Li/Li^+),[45] whereas the 2SM3/LiBOB system decomposes at potentials more positive than 4.2 V vs Li/Li^+.[46] These results imply that there is a window of approximately 3.2 V over which the system is stable. This agrees with our observation that the two-electrode cells using VACNF electrodes are stable up to approximately 3.0 V.

Recent studies showed that at high applied potentials, the decomposition of LiBOB created a self-terminated surface layer.[14] Our results show that this layer passivates the surface against further decomposition and thereby allows stable charge storage at cell voltages up to 5 V. Moreover, this is stable upon repeated cycling of the voltage. Figure 6, for example, shows that the resulting interfaces have a capacitance that is stable through >800 cycles between 0 and 5 V. An initial decrease likely arises from the formation of this passivating layer. Although this time is short compared to what is needed for many practical applications, these data suggest that organosilicon electrolytes such as 2SM3 may be useful materials for use in energy storage applications.

Additionally, because organosilicon electrolytes are much less flammable than the organic electrolytes currently in use,[12] their use may provide an additional element of safety in applications where large amounts of energy must be stored. A very recent study has shown that 2SM3 shows no decomposition until temperatures of >130 °C; in addition, the organosilicon electrolyte leads to better cathode stability comparing with conventional carbonate-based electrolyte.[46]

5. Conclusions

We have demonstrated that vertically aligned carbon nanofibers with a model organosilicon electrolyte yield interfaces that exhibit high interfacial capacitance over a wide range of applied voltages. We demonstrate that the exposure of edge-plane graphite along the sidewalls of the nanofibers yields electrodes exhibiting a high degree of metallic character that results in high interfacial capacitance. The increase of ~20 times for nanofibers compared with planar electrodes is comparable to the increase in surface area, indicating that the sidewall of the VACNF electrodes are effective at creating electrical double-layers. The interfacial capacitance has only a weak frequency dependence, demonstrating excellent accessibility to the nanofiber sidewalls without diffusion limitations. Our data show that the interfaces between organosilicon electrolytes and nanostructured carbon materials can effectively take advantage of the high stability of the organosilicon electrolytes and the high surface area of nanostructured electrodes. Because nanofiber length can be further increased using longer deposition times,[20] additional increases in microscopic surface area should be possible. The results imply that the carbon nanofibers and organosilicon electrolytes have potential in various energy applications such as photoelectrochemical cells, batteries, and double layer capacitors.

Acknowledgment. This work was supported by the National Science Foundation Grants CHE0613010, DMR0210806, and DMR0425880.

CM0714842

(42) Kim, Y.-J.; Horie, Y.; Matsuzawa, Y.; Ozaki, S.; Endo, M.; Dresselhaus, M. S. *Carbon* **2004**, *42*, 2423.
(43) Hughes, M.; Chen, G. Z.; Shaffer, M. S. P.; Fray, D. J.; Windle, A. H. *Chem. Mater.* **2002**, *14*, 1610.
(44) Niu, C. M.; Sichel, E. K.; Hoch, R.; Moy, D.; Tennent, H. *Appl. Phys. Lett.* **1997**, *70*, 1480.
(45) Xu, K.; Lee, U.; Zhang, S.; Jow, T. *J. Electrochem. Soc.* **2004**, *151*, A2106.
(46) Nakahara, H.; Tanaka, M.; Yoon, S.; Nutt, S. *J. Power Sources* **2006**, *160*, 645.